High Pressure Torsion: from Laminar Flow to Turbulence

To cite this article: R Kulagin *et al* 2017 *IOP Conf. Ser.: Mater. Sci. Eng.* **194** 012045

IOP Conf. Series: Materials Science and Engineering **194** (2017) 012045 doi:10.1088/1757-899X/194/1/012045

High Pressure Torsion: from Laminar Flow to Turbulence

R Kulagin[1], Y Beygelzimer[2], Y Ivanisenko[1], A Mazilkin[1,3] and H Hahn[1]

[1]Institute of Nanotechnology (INT), Karlsruhe Institute of Technology (KIT), Hermann-von-Helmholtz-Platz 1, 640, 76344 Eggenstein-Leopoldshafen, Germany
[2]Donetsk Institute for Physics and Engineering named after O.O. Galkin, NASU, Vernadsky Str. 46, 03142 Kyiv, Ukraine
[3]Institute of Solid State Physics, RAS, Academician Ossipyan Str.2, 142432 Chernogolovka, Russia

roman.kulagin@kit.edu

Abstract. We analyzed experimentally and theoretically deviations from the simple High Pressure Torsion (HPT) scheme. We showed that the nature of the plastic flow and the deformed state of the sample under HPT depends on the structure and mechanical properties of the material being processed. Both laminar and turbulent flows under HPT were analysed. It was demonstrated that non-laminar flow causes intensive mass transfer and mixing of the deformed material. As an example, mechanical synthesis of the high entropy alloys from elemental powders by HPT is presented.

1. Introduction

High Pressure Torsion (HPT) is a widely used process for modifying the materials structure and properties by means of severe plastic deformation [1]. It is a generally accepted assumption that deformation during HPT occurs by simple shear. The shear is uniform over the sample's thickness and shear strain γ at each point of the sample is proportional to the distance r from the anvil rotation axis and to the rotation angle β:

$$\gamma = \frac{r\beta}{t} \tag{1}$$

where t is the sample thickness.

Experiments and numerical simulations in recent years show that the actual plastic flow during HPT may differ significantly from this simple scheme. The influence of the geometric parameters and conditions of contact friction during the HPT deformation on the spatial strain distribution in the sample's bulk was studied in [2–5]. In [6] the dependence of the strain rate field on the stress-strain curve and rotation angle was investigated.

It was shown that if the strain hardening obeys the power-law and the strain-rate hardening is absent, the strain rate field in the sample volume is independent on the anvil rotation angle. In this case, the value of shear strain at any point of the sample is proportional to the rotation angle. Any deviation from the aforementioned conditions results in the unsteadiness of the strain rate field. The latter means that shear strain ceases to depend linearly on the rotation angle. It was also shown in [6] that when strain hardening is saturated and the strain-rate hardening is absent, then the strain is concentrated in a thin layer of the sample. This effect is not related to the geometry of the anvils or friction, but is rather determined by instability of the material during the plastic shear deformation [7, 8].

We show it in Section 2 of this work that certain adjustments to the conclusions of [6] have to be made if strain-rate hardening is to be considered. On increasing the magnitude of the strain-rate hardening, the thickness of the layer where the deformation is concentrated becomes progressively larger until no localization is observed. When the strain-rate hardening stops to increase, the strain-rate field approaches a steady state and shear deformation depends linearly on the rotation angle β.

We carried out HPT deformation experiments on copper samples with aluminum markers (see Section 3). The experiments showed that at sufficiently large strains the two materials (Cu and Al) were intermixed. We regard this result as an evidence of transition from laminar to turbulent flow in the material under HPT deformation. This transition corresponds to the two-stage simple shear hypothesis [9].

2. Dependence of the strain-rate field on the anvil rotation angle

It was shown in [10] that the saturation of strain hardening during HPT should lead to strain localization in a thin layer of the sample if the strain-rate hardening is absent [6]. We will show by means of FEM computer simulations that in this case strain-rate hardening may stabilize the plastic flow at HPT and prevent strain localization.

All calculations were done with the DEFORM – 2D/3D software using a 2D axisymmetric torsion model [11]. The set-up for the HPT experiment is shown in figure 1a

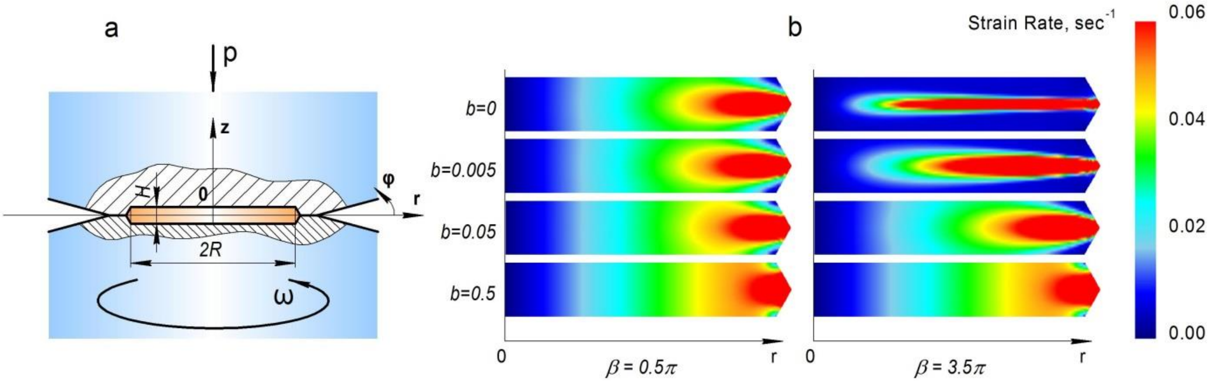

Figure 1. To the calculation of the strain-rate field during HPT: (a) schematic geometry of HPT, (b) von Mises strain rate maps for a horizontal plane at two different anvil rotation angles (FEM simulation); values of the strain-rate are indicated in the figure. The parameter b is defined in the text below.

The stress-strain curve was specified by the following power-law relation:

$$\sigma_S[MPa] = \sigma_S^*(e_M)\cdot\left(\frac{\dot{e}_M}{a}\right)^b \tag{2}$$

where $\sigma_S^*(e_M)$ is the experimental dependence for powder iron [6] and a and b are strain-rate hardening parameters.

For the calculations the value of a was assumed to be equal to 0.05s^{-1}. We studied the evolution of the strain rate field depending on the b value for b equal to 0, 0.005, 0.05 and 0.5. In all experiments, the sample diameter was 10 mm, and its thickness was 1 mm.

The results of the calculations are shown in figure 1b. It is seen that, as the b parameter increases, the area of large shear deformation becomes broader. Ultrafine-grained materials processed by HPT usually have strain rate sensitivity coefficient in the range of 0.01 - 0.1 [13, 14]. This means that equation (1) can still be applied as a rough estimate for the shear strain during HPT. However, it should be noted that the area of large deformation may be reduced. The reason is that the saturation of strain hardening when the value of strain-rate hardening may be incomplete.

3. Turbulent flow of the material during HPT

This section describes the results of HPT experiments on Cu samples containing inserts of Al and brass markers. Samples were prepared as follows. Eight 2 mm channels were drilled in Cu cylinder having the length of 35 mm and the diameter of 20 mm. The channels were drilled at a distance of 4.0 and 7.0 mm from the axis of the workpiece. The Al wire was inserted into four channels which were closer to the axis of the cylinder. Brass wire was put into the peripheral channels. The workpiece was subjected to direct extrusion and its diameter shrank to 12 mm to seal the wires in copper matrix. Disc-shaped specimens 1 mm in thickness were cut from the workpiece. We used these disks for HPT experiments. Deformation was performed at a pressure of 4.5 GPa and an angular velocity of the anvils of 1 revolution per minute. Figure 2 shows sections of the samples normal to the rotation axis after the rotation to angles $\pi/2$ (figure 2a) and π (figure 2b).

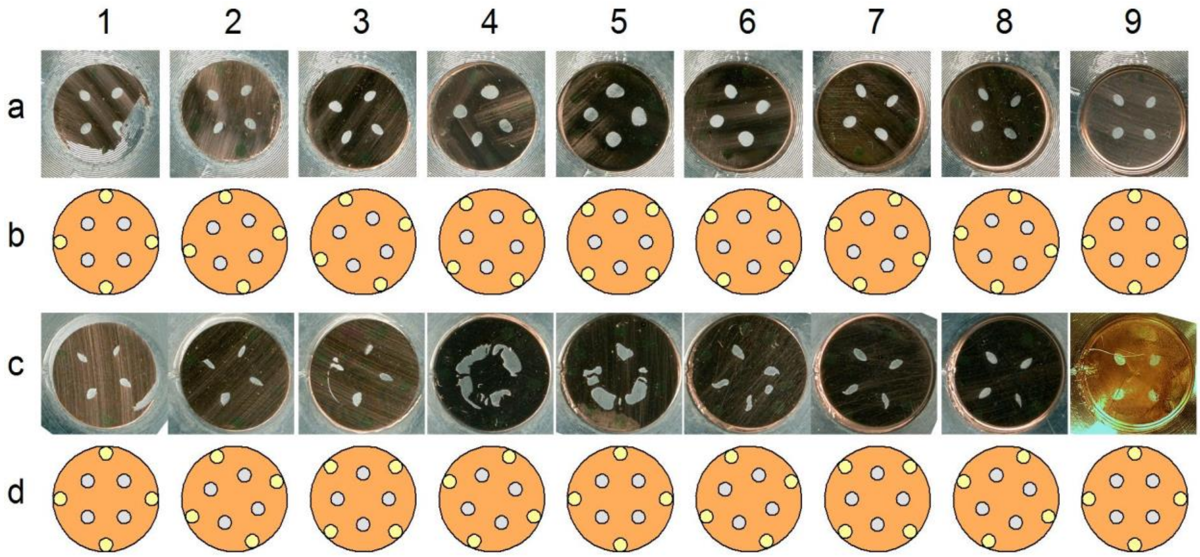

Figure 2. Rotation to 90° (a and b); rotation to 180° (c and d). Numbers in figure correspond to the depth step (each step is 100 μm).

Figure 2a, b shows that when $\beta = \pi/2$ the positions of the markers coincide well with those calculated from the model of the simple shear deformation. This indicates the validity of this model, at least for this value of the rotation angle. The picture changes completely for $\beta = \pi$. The markers are blurred for the depths from 300 to 500 μm (figure 2c, d). This suggests that the major deformation is localized in this 300 μm thick layer. The cross-section of an HPT deformed disk after three revolutions of the anvils is shown in figure 3. It can be seen from the figure that HPT leads to the mixing of the material of the matrix with that of the markers.

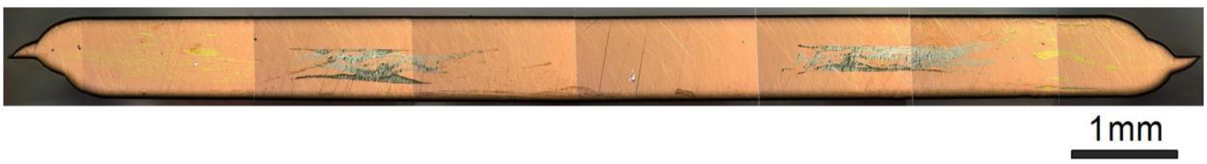

Figure 3. Cross-section of a Cu disk with markers after HPT deformation; three revolutions of the anvils were performed.

This mixing is possible only in the presence of turbulent eddy currents in the sample during HPT. This conclusion is consistent with the suggestions of the authors [9] that turbulent flow takes place in the material at large simple shear strains. We suppose that it is the turbulent plastic flow which explains the efficiency of HPT for the cold fusion of various materials in the first works of Bridgman [15]. Formation of the alloys is associated with the mass transfer by the diffusion mechanism. The diffusion can be rather fast at elevated temperature, but the rate of the diffusion mass transfer at low temperature is not high enough. The rate of the mass transfer necessary for cold fusion can be provided only by a stochastic vortex motion, which is similar to the turbulent flow in liquids or gases. The next section of this paper will show that HPT processing of a powder mixture of a certain composition results in the formation of high entropy alloys at ambient temperatures. We believe that a turbulent flow of the material during the HPT deformation plays the most important role in this process.

In [20] the formation of vortices in the plastically deformed material under simple shear is associated with a local blocking of the shear deformation. Let us show by numerical modeling that the local blocking of the shear deformation in the sample under HPT leads to the twists and turns of the obstacles. We regard this as the physical cause for the turbulent flow during the HPT.

Figure 4 shows the scheme and the results of calculations. Layer of plastic material is located between the two plates, moving in opposite directions. There are obstacles in the layer, locally locking the shear. The obstacle is of the material with the yield stress ten times higher than that in the layers and it has the shape of a cylinder (perpendicular to the plane of the figure).

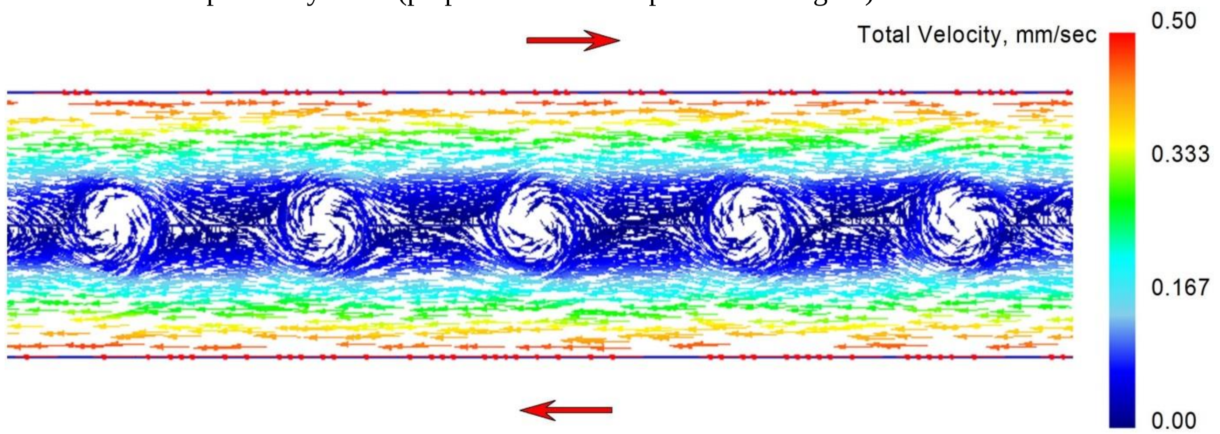

Figure 4. Simple shear blocked locally by the obstacles (FEM simulation).

Figure 4 shows that the local blocking of the shear really causes rotation of obstacles, which leads to the formation of vortices at sufficiently large shear strain. As obstacles during the HPT deformation, non-uniformities in the material of different kinds may be considered.

4. Obtaining high entropy alloy by turbulent flow during HPT

A high entropy CoCrMnFeNi alloy was produced from a mixture of powders by means of high pressure torsion. To prepare this mixture, we used powders of Co(>99.8 wt%), Cr (>99.2 wt%), Mn (>99.6 wt%), Fe (>99.5 wt%) and Ni (>99.9 wt%) with the size of about 1-10 μm. The mixture prepared for the HPT treatment contained equal atomic fractions of all components. The treatment was carried out in a custom built computer-controlled HPT device using flat anvils under the following conditions: the applied pressure P=5 GPa, anvils rotation speed ω=5 rpm and number of rotations N=100. The temperature in the deformation zone was monitored by the laser pyrometer and it was ~200°C.

The obtained sample was investigated in a TITAN 80–300 transmission electron microscope (TEM). The sample for the investigation was prepared using a FEI Strata 400S dual beam facility. The results of the investigations are presented in figure 5.

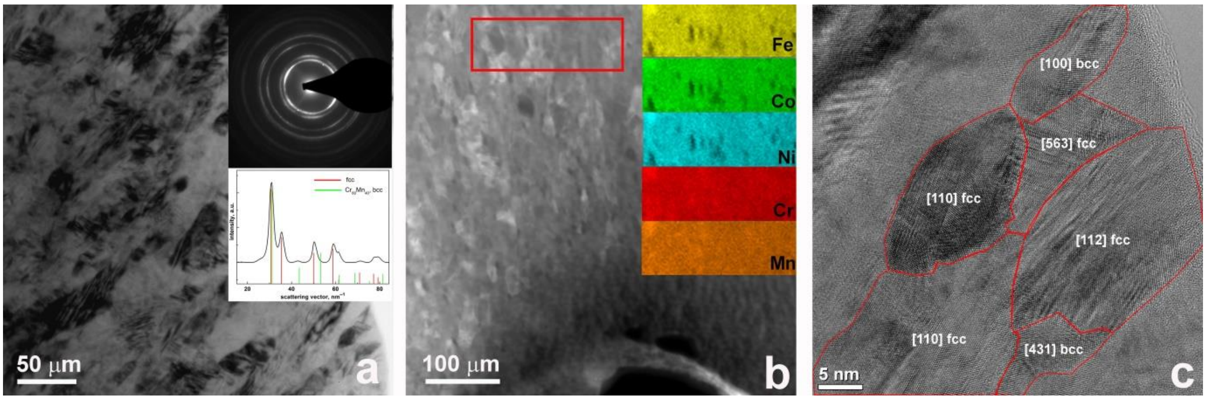

Figure 5. Microstructure analysis of the CoCrMnFeNi alloy after HPT: (a) bright field image (in the inserts are a selected area electron diffraction (SAED) pattern and a corresponding intensity radial distribution plot). Vertical lines denote the positions of the reflections from CoCrMnFeNi fcc phase (red) and $Cr_{60}Mn_{40}$ bcc phase (green) correspondingly); (b) HAADF STEM image with the elemental maps for Fe, Co, Ni, Cr and Mn as inserts; (c) high resolution TEM image of the grain structure (red lines denote the boundaries between the grains of different phases with indexed normal orientations).

According to the results presented in figure 5, the HPT treatment of the mixture of individual powder particles resulted in the formation of the CoCrMnFeNi alloy. It follows from the obtained results that the alloy consists mainly of the fcc phase although the particles of second phase are also observed in the structure. According to the SAED, the second phase is $Cr_{60}Mn_{40}$ bcc phase (W structure type). This conclusion is also supported by the results of elemental mapping (figure 5b). It can be seen that all the elements are distributed homogeneously over the sample, with the exception of small areas about 10 nm in size, which are mostly composed of Cr and Mn. We can estimate the volume fraction of bcc phase to be as high as 7 %. High resolution TEM image (figure 5c) shows the grain structure of the obtained alloy. From this image the grain size can be estimated at about 20 nm. The mechanism of the solid-state HEA alloy formation is not the purpose of this study. Irrespective of what this mechanism is, it is related to the intensive mass transfer. As stated earlier, we suppose that it is the turbulent flow that ensures the mass transfer.

Conclusions

The results obtained indicate that the mechanical properties and the structure of the processed materials can have a significant effect on the velocity field and strain state in a sample process by HPT. At stress saturation in a material with low or zero strain-rate hardening, the deformation is localized in a thin layer of the sample. The thickness of this layer increases with increasing exponent b of strain-rate hardening. For $b > 0.1$ no strain localization occurs. The occurrence of strain non-uniformities inhibiting simple shear leads to a turbulent flow pattern under HPT. This accelerates the mass transfer required for the formation of alloys. We show in our study that the HEA alloys can be obtained by means of this approach.

Acknowledgment

YB would like to express his gratitude to the State Fund for Fundamental Research of the Ukraine for financial support of research on vortex flow under twist extrusion through the competitive grant F71/56-2016.

References

[1] Zhilyaev A P and Langdon T G 2008 *Prog. Mater Sci.* **53** 893
[2] Figueiredo R B, Faria G C V, Cetlin P R and Langdon T G 2013 *J. Mater. Sci.* **48** 4524

IOP Conf. Series: Materials Science and Engineering **194** (2017) 012045 doi:10.1088/1757-899X/194/1/012045

[3] Yoon S C, Horita Z and Kim H S 2008 *J. Mater. Process. Technol.* **201** 32
[4] Pippan R, Scheriau S, Hohenwarter A and Hafok M 2008 *Mater. Sci. Forum* **584-586** 16
[5] Lee D J and Kim H S 2014 *J. Mater. Sci.* **49** 6620
[6] Beygelzimer Y, Kulagin R, Toth L S and Ivanisenko Y 2016 *Beilstein J. Nanotechnol.* **7** 1267
[7] Hill R 1958 *J. Mech. Phys. Solids* **6** 236
[8] Beigelzimer Y, Efros B, Varyukhin V and Khokhlov A 1994 *Eng. Fract. Mech*. **48** 629
[9] Beygelzimer Y, Valiev R Z and Varyukhin V 2011 *Mater. Sci. Forum* **667-669** 97
[10] Beygelzimer Y, Toth L S and Jonas J J 2015 *Adv. Eng. Mater*. **17** 1783
[11] DEFORM *Scientific Forming Technologies Corporation* http://www.deform.com/
[12] Zhao Y J, Massion R, Grosdidier T and Toth L S 2015 *Adv. Eng. Mater*. **17** 1748
[13] Chinh N, Szommer P, Horita Z and Langdon T 2006 *Mater. Sci. Forum* **503–504** 1001
[14] Valiev R Z, Murashkin M, Kilmametov A, Straumal B, Chinh N and Langdon T 2010 *J. Mater. Sci*. **45** 4718
[15] Bridgman P W 1935 *Phys. Rev*. **48** 15.
[16] Panah M P 2015 *Shear-Induced Mixing in Metallic Systems, PhD Thesis* (Darmstadt, Germany)
[17] Kim H J, Karthikeyan S and Rigney D 2009 *Wear* **267** 1130
[18] Sundaram N K , Guo Y and Chandrasekar S 2012 *Phys. Rev. Lett*. **109** 106001
[19] Prandtl L and Tietjens OG 1957 *Fundamentals of Hydro - and Aeromechanics*, (New York: Dover Pub. Inc.)
[20] Beygelzimer Y 2011 *Mater. Sci. Forum* **683** 213